Synthesis and Characterization of Side-Chain Cholesteric Liquid-Crystalline Polysiloxanes Containing Different Space Groups

Ji-Wei Wang, Fan-Bao Meng, Yuan-Hao Li, Bao-Yan Zhang

The Research Centre for Molecular Science and Engineering, Northeastern University, Shenyang 110004, People's Republic of China

Received 10 September 2007; accepted 7 July 2008
DOI 10.1002/app.29214
Published online 10 November 2008 in Wiley InterScience (www.interscience.wiley.com).

ABSTRACT: A series of liquid-crystalline (LC) polysiloxanes were synthesized by two different cholesteric monomers, cholest-5-en-3-ol(3β)-10-undecenoate and cholesteryloxycarbonylmethyl 4-allyloxybenzoate. The chemical structures and LC properties of the monomers and polymers were characterized by various experimental techniques, including Fourier transform infrared spectroscopy, ^{1}H-NMR, elemental analysis, differential scanning calorimetry, and polarized optical microscopy. The specific rotation absolute values increased with increasing rigid spacers between the main chain and the mesogens. All of the polymers exhibited thermotropic LC properties and revealed cholesteric phases with very wide mesophase temperature ranges. With a reduction in the soft-space groups in the series of polymers, the glass-transition temperature and the isotropic temperature increased slightly on heating cycles. Reflection spectra of the cholesteric mesophase of the series of polymers showed that the reflected wavelength shifted to short wavelengths with decreasing soft-space groups in the polymers systems, which suggested that the helical pitch became shorter with increasing rigid-space groups. © 2008 Wiley Periodicals, Inc. J Appl Polym Sci 111: 2078–2084, 2009

Key words: chiral; liquid-crystalline polymers (LCP); polysilanes

INTRODUCTION

Side-chain liquid-crystalline polymers (LCPs) combine the electrooptical properties of low-molecular-weight liquid crystals with the mechanical properties and easy processing of polymers.[1–4] Recently, a focus of interest in the synthesis of LCPs has been the preparation of chiral LCPs. Chirality has become one of the most important and complex topics in liquid-crystal research. This is mainly due to the fact that molecular asymmetry imparts form chirality to the liquid-crystalline (LC) phases and leads to possible new technical applications for chiral LCPs.[5–10]

Chiral LCPs may exhibit a marvelous variety of LC phases, including the chiral smectic C* phase, the cholesteric phase, and the blue phases. Cholesteric liquid crystals are chiral nematics, where the handedness of the constituent molecules causes the orientation of the local nematic director to vary in space. In the helical cholesteric structure, the director is perpendicular to the helix axis. On the other hand, orientation varies linearly along the helix axis. The spatial period of the structure is the pitch, which is determined by the concentration and the helical twisting power of the chiral constituents. As a result of the periodicity of the helical cholesteric structure and the birefringence of the liquid crystal, for a range of wavelengths, light propagation along the helix axis is forbidden for one of the normal modes. Because propagation is forbidden, incident light with a wavelength in this band and with the same helicity as the cholesteric is strongly reflected. The edges of this reflection band are at wavelengths that are equal to the refractive indices times the pitch. If the reflected wavelength is in the visible range of the spectrum, the cholesteric phase appears colored. Cholesteric LCPs with the unique property of selective reflection of circularly polarized light have presented large potential for various optical applications.[11–20]

We are interested in chiral LCPs prepared with chiral LC monomers and other polymerizable groups. Because of the large potential for various optical applications of chiral LCPs, it is important to study the optical properties of LCPs containing

Correspondence to: B.-Y. Zhang (byzcong@163.com).
Contract grant sponsor: National Natural Science Fundamental Committee of China.
Contract grant sponsor: China Postdoctoral Science Foundation.
Contract grant sponsor: Educational Science and Technology Program of Liaoning Province (Education Department and Science and Technology Department of Liaoning Province).

© 2008 Wiley Periodicals, Inc.

chiral mesogens. In this study, a series of polysiloxane-based cholesteric LCPs were graft-polymerized by two different cholesteric LC monomers.

EXPERIMENTAL

Materials and measurements

4-Hydroxybenzoic acid, 3-bromopropene, potassium hydroxide, hydroxylacetic acid, cholesterol, hexachloroplatinic acid hydrate, and poly(methylhydrogeno)siloxane (PMHS; number-average molecular weight = 600–800) were obtained from Jilin Chemical Industry Co. (Jilin City, China) and were used without further purification. Pyridine, thionyl chloride, chlorethyl alcohol, toluene, ethanol, chloroform, tetrahydrofuran (THF), and methanol were purchased from Shenyang Chemical Co. (Shenyang City, China) Pyridine was purified by distillation over KOH and NaH before use.

Fourier transform infrared (FTIR) spectra of the synthesized polymers and monomers in the solid state were obtained by the KBr method performed on a PerkinElmer Spectrum One spectrometer (PerkinElmer, Foster City, CA). ^{1}H-NMR (300-MHz) spectra were obtained with a Varian WH-90PFT NMR spectrometer (Varian Associates, Palo Alto, CA) with Fourier transform with dimethyl sulfoxide-d_6 or $CDCl_3$ as the solvent and tetramethylsilane as the internal standard. Elemental analyses were carried with an Elementar Vario EL III (Elementar, Hanau, Germany). Thermal transition properties were characterized by a Netzsch instruments DSC 204 (Netzsch, Wittelsbacherstr, Germany) at a heating rate of 10°C/min under a nitrogen atmosphere. Phase-transition temperatures were collected during the second heating and the first cooling scans. Visual observation of the LC transitions and optical textures under cross-polarized light was made by a Leica DMRX polarized optical microscope (Leica, Wetzlar, Germany) equipped with a Linkam THMSE-600 hot stage (Linkam, Surrey, England). Ultraviolet–visible spectrophotometry was measured by PerkinElmer Lambda 950 instrument. X-ray measurements of the samples were performed with Cu Kα radiation (wavelength = 1.542 Å) monochromatized with a Rigaku DMAX-3A X-ray diffractometer (Akishima, Tokyo, Japan). Measurements of optical rotation were carried out with a PerkinElmer model 341 polarimeter at different temperatures of heating and cooling cycles with a sodium light source (wavelength = 589 nm).

Synthesis of the monomers

The LC monomer cholest-5-en-3-ol(3β)-10-undecenoate (**M1**) and the intermediate 4-allyloxybenzoyl chloride (**1**) were prepared according to previous reports.[4,21] The synthesis routes of the polymers and the chiral LC monomer cholesteryloxycarbonylmethyl 4-allyloxybenzoate (**M2**) are shown in Scheme 1.

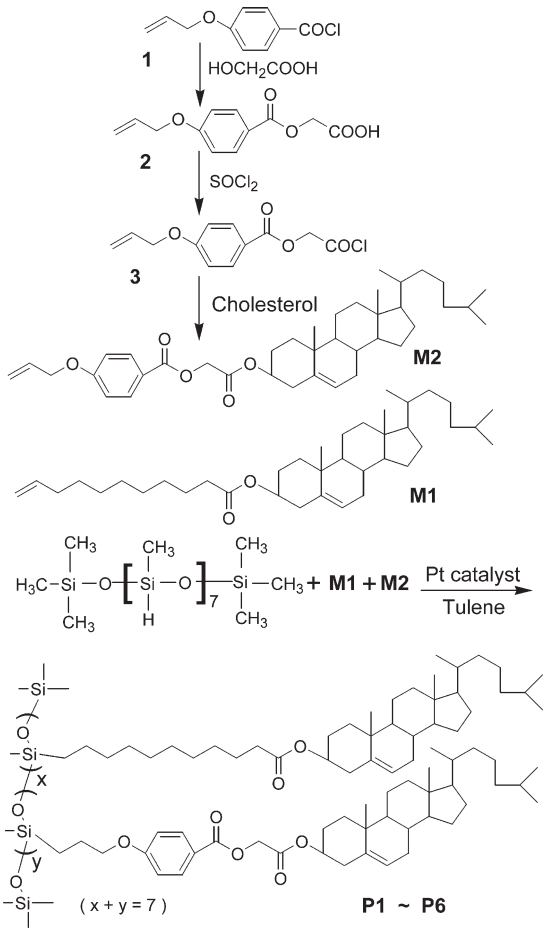

Scheme 1 Synthesis routes of the chiral LC monomers and the polymers.

Hydroxylacetic acid (15.2 g, 0.2 mol) and pyridine (3.0 mL) were dissolved in 45 mL of THF. This was added dropwise to 60 mL of a dry THF solution containing **1** (27.6 g, 0.20 mol) and 0.5 mL of pyridine. The reaction mixture was stirred at 60°C for 8 h. Some solvent was distilled under reduced pressure. After it was cooled to room temperature, the mixture was poured into 1000 mL of cold water. The precipitates were isolated by filtration, washed with hot water, recrystallized in alcohol, and dried in a vacuum oven to obtain white crystals of carboxymethyl 4-allyloxybenzoate (**2**).

The intermediate **2** (28.4 g, 0.10 mol), thionyl chloride (60 mL), and pyridine (1.0 mL) were added to a round flask equipped with an absorption instrument of hydrogen chloride. The mixture was stirred at room temperature for 3 h, then heated to 60°C, and kept for 6 h in a water bath to ensure that the reaction finished. The excess thionyl chloride was distilled under reduced pressure. Then, 100 mL of cold THF was added to the residue at 20°C to obtain a

TABLE I
Polymerization, Specific Rotation, and Maximum Selective Reflection Wave Number (λ_{max}) Values of the Polymers

Sample	Feed			Integration ratio of Ar—*H*/Si—C*H*$_3$ signals[a]	Mesogens with rigid space groups (wt %)[b]	λ_{max} (nm)[c]	$[\alpha]_D^{20}$[d]
	PMHS (mmol)	**M1** (mmol)	**M2** (mmol)				
P1	0.2857	1.80	0.20	0.057	7.5	698	−5.988
P2	0.2857	1.60	0.40	0.129	16.8	677	−5.848
P3	0.2857	1.20	0.80	0.258	33.2	656	−5.419
P4	0.2857	0.80	1.20	0.402	50.9	639	−5.376
P5	0.2857	0.40	1.60	0.531	66.3	625	−4.921
P6	0.2857	0	2.00	0.718	87.9	599	−4.303

[a] Determined by ^{1}H-NMR analysis.
[b] Calculated value according to the **M2** substitution degree as derived from ^{1}H-NMR analysis.
[c] At 100°C.
[d] 0.1 g in 10 mL of $CHCl_3$.

THF solution of chlorocarbonylmethyl 4-allyloxybenzoate (**3**).

Cholesterol (38.7 g, 0.1 mol) and of pyridine (18 mL) were dissolved in 350 mL of dry THF. This was added dropwise to a THF solution of **3** (60.5 g, 0.20 mol). The reaction mixture was stirred at 65°C for 8 h. The solvent was distilled out partly under reduced pressure. After cooling to room temperature, the mixture was poured into 1200 mL of cold water. The precipitates were isolated by filtration and dried in a vacuum oven. Recrystallization in alcohol resulted in white crystals of the LC monomer **M2**.

Yield = 7%. $[\alpha]_D^{20} = -43.2°$, $c = 1$, chloroform; mp = 29°C. IR (KBr, cm^{-1}): 3076, 2926, 2860 (CH_3—, —CH_2—, —CH—, Ar—H); 1765, 1724 (C=O); 1608, 1506 (Ar). ANAL. Calcd for $C_{39}H_{56}O_5$: C, 77.44%; H, 9.33%. Found: C, 77.63%; H, 9.22%. ^{1}H-NMR ($CDCl_3$, δ, ppm): 0.73–2.15 (m, 44H, alkyl—*H*), 3.70–3.98 (m, 1H, —OC*H*—), 4.69–5.48 (m, 2H, C*H*$_2$=CH—), 5.60–5.78 (m, 4H, —OC*H*$_2$—), 6.02–6.17 (m, 1H, CH_2=C*H*—), 6.93–7.85 (m, 4H, Ar—*H*).

Synthesis of the polymers

For synthesis of polymers **P1–P6,** the same method was adopted. The polymerization experiments and yields are summarized in Table I. The synthesis of polymer **P4** is given as an example. Chiral LC monomer **M1** (0.80 mmol) was dissolved in 60 mL of dry, fresh distilled toluene. To the stirred solution, the LC monomer **M2** (1.20 mmol), PMHS (0.2857 mmol), and 2 mL of H_2PtCl_6/THF (0.50 g of hexachloroplatinic acid hydrate dissolved in 100 mL of THF) were added and heated under nitrogen and anhydrous conditions at 65°C for 48 h. Some solvent was removed under reduced pressure, cooled, and poured into methanol. After filtration, the product was dried at 80°C for 2 h *in vacuo* to obtain 2.14 g of polymer.

Yield = 90%. IR (KBr, cm^{-1}): 2964–2874 (CH_3— and —CH_2—); 1754–1720 (C=O); 1608, 1510 (Ar); 1261, 1191–1084 (Si—O—Si). ^{1}H-NMR ($CDCl_3$, δ, ppm): 0.18–0.38 (m, 4.72H, Si—C*H*$_3$), 1.28–2.68 (m, 45.65H, —C*H*$_2$—), 3.72–3.96 (m, 0.98H, —OC*H*—), 5.38–5.52 (m, 1.91H, —OC*H*$_2$—), 6.97–7.44 (m, 1.90H, Ar—*H*).

RESULTS AND DISCUSSION

Syntheses

The synthetic routes for the target monomer **M2** are shown in Scheme 1. The structures of **M2** were characterized by IR and ^{1}H-NMR spectroscopy, which was in good agreement with the prediction. The spectra of **M2** suggested that the purity was high, and this was confirmed by elementary analysis.

Polymers **P1–P6** were prepared by a one-step hydrosilylation reaction between the Si—H groups of PMHS and the olefinic C=C of **M1** and **M2** in toluene with hexachloroplatinic acid as a catalyst. The obtained polymers were soluble in toluene, xylene, THF, chloroform, and so forth. Their structures were characterized by IR and ^{1}H-NMR spectroscopy. Polymer **P4** contained the representative features of all of the polymers. Their characteristic absorption bands were as follows: 2964–2874 (C—H stretching), 1754–1720 (C=O stretching in different kinds of ester modes), 1608 and 1510 (aromatic stretching), and 1191–1084 cm^{-1} (Si—O—Si stretching). The disappearance of the PMHS Si—H stretching at 2160 cm^{-1} and the olefinic C=C stretching band at 1635 cm^{-1} indicated the successful incorporation of monomers into the polysiloxane chains. In addition, the ester C=O absorption bands of monomers **M1** and **M2** and the characteristic Si—O—Si broad stretching bands of PMHS still existed in the polymers. FTIR spectra of the polymers are shown in Figure 1. With increasing **M2** in the polymer systems, the aromatic stretching peaks at 1608 and

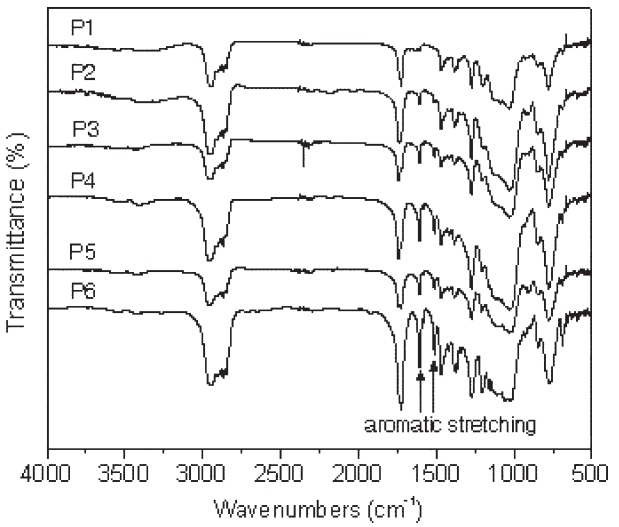

Figure 1 FTIR spectra of polymers **P1–P6**.

1510 cm^{-1} increased, which suggested an increase in the mesogens with rigid-space groups. However, the components of the mesogens with rigid-space groups could not be calculated by FTIR spectroscopy.

For the LC polysiloxanes, it was necessary to know the polymer composition and molecular weights. Therefore, we performed NMR analyses of the polymers, taking into consideration their solubility in chloroform. The ^{1}H-NMR spectrum of **P4** and its chemical structure were shown previously. For PMHS, the substitution degree was determined by comparison of the integration of the Si—H signals to those of the Si—methyl groups. The δ of —SiH— was 4.55–4.68 ppm for PMHS in the ^{1}H-NMR spectrum of PMHS, but there were no peaks at δ = 4.55–4.68 ppm for any of the polymers. These results indicate that all of the Si—H groups in PMHS were substituted via the hydrosilylation action and that the monomers were connected to the polysiloxane chains. To determine the polymer composition, the **M2** substitution degree was determined by comparison of the integration ratio of the Ar—*H*/Si—CH_3 signals by ^{1}H-NMR analyses in the polymer systems because the **M1** component showed no Ar—*H* signals. Therefore, the composition of the polymers and the components of the mesogens with rigid-space groups were calculated; these are listed in Table I.

The optical properties of chiral LCPs result from chiral molecules in the LC state that induce a twist in the direction of adjacent molecules, which thereby forms a supermolecular helical structure. Therefore, it is interesting to study the variation of optical rotation due to introduction of different chiral groups in the side-chain LCPs. Although the specific rotations of the chiral LCPs were all negative, the cleavage of the double bond and the binding of two monomers to the polysiloxane main chains seemed to significantly affect the chirality of the compounds, as shown in Table I. Compared with the monomers, the polymers showed significantly lower specific rotations. The results suggest that the existence of polysiloxane main chains affected the molecular polarity, which led to a decrease in the specific rotations. As shown in Table I, the specific rotations of polymers **P1–P6** revealed similar tendencies; that is, the specific rotation absolute values decreased with increasing mesogens with rigid-space groups in the polymer systems. This was due to different spacers between the main chain and the mesogens.

Thermal analysis

The differential scanning calorimetry (DSC) thermograms of **M2** in the heating and cooling cycles are presented in Figure 2. The DSC curves of **M2** showed a melting transition and a cholesteric–isotropic phase transition at 129.3 and 236.8°C, respectively, on heating and displayed an isotropic–cholesteric phase transition and a crystallization process at 152.1 and 96.8°C, respectively, on cooling.

The phase-transition temperatures of **P1–P6** obtained from the second heating and the first cooling scan are summarized in Table II. Some representative DSC thermograms of the polymers are shown in Figure 3. All phase transitions were reversible and did not change on repeated heating and cooling cycles. The phase-transition temperatures determined by DSC were consistent with the polarized optical microscopy (POM) observation results.

The DSC thermograms of **P1–P6** showed a glass transition and a LC phase to isotropic transition. The effect of the components of mesogens with rigid-space groups on the transition temperature of the LC phases on heating cycles is shown in Figure 4.

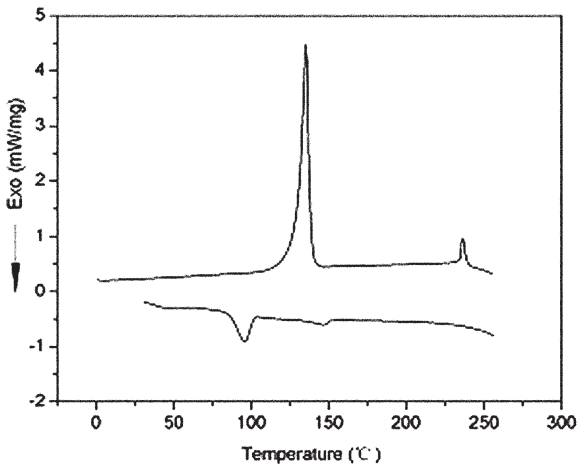

Figure 2 DSC thermograms of monomer **M2** on the second heating and the first cooling.

TABLE II
DSC Results for the Polymer Series

	Heating			Cooling	
Sample	T_g (°C)	T_i (°C)	ΔT (°C)[a]	T_{i-N} (°C)[b]	T_{N-K} (°C)[c]
P1	16.3	189.1	172.8	186.1	14.2
P2	16.8	192.3	175.5	191.9	15.6
P3	17.0	205.4	188.4	205.6	16.8
P4	19.9	206.6	186.7	204.8	17.9
P5	23.7	207.2	183.5	205.1	18.3
P6	26.5	208.4	181.9	206.7	21.3

[a] Mesophase temperature range (T_i–T_g).
[b] Phase transition from isotropic state to mesophase.
[c] Phase transition from mesophase to solid.

For polymers **P1–P6,** the glass-transition temperature (T_g) and the isotropic temperature (T_i) increased slightly on heating cycles with increasing mesogens with rigid-space groups. LCPs are most commonly composed of flexible and rigid moieties, the polymer backbone; the rigidity of the mesogenic units and the length of the flexible spacer influence the mesophase behaviors of the polymers. Because of the same polymer backbone and different lengths of the flexible spacers in **M1** and **M2**, all of the polymers displayed increasing T_g values with increasing rigid-space groups components in the polymer systems.

Texture analysis

The optical textures of the monomers and polymers were studied by means of POM with a hot stage. The POM results show that **M2** exhibited an enantiotropic cholesteric phase in the heating and cooling cycles. When **M2** was heated, the typical cholesteric oily streak texture appeared, as shown in Figure 5(a,b). Different colors correspond to different twist states. When the isotropic state was cooled, the cholesteric droplet and fan-shaped texture appeared.

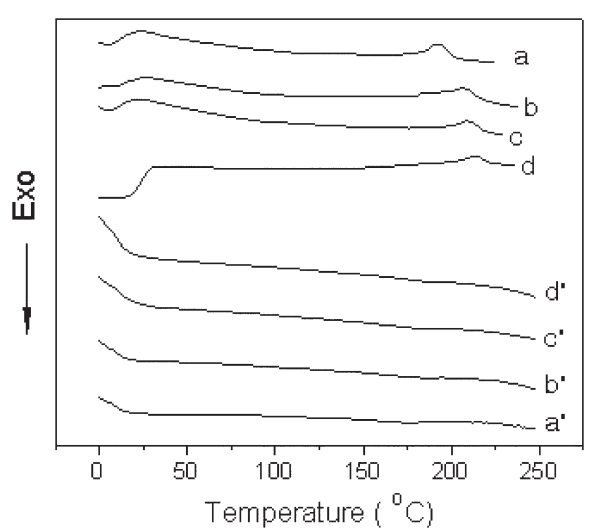

Figure 3 DSC thermograms of representative polymers: (a) **P2**, (b) **P3**, (c) **P4**, and (d) **P6** on the second heating and (a′) **P2**, (b′) **P3**, (c′) **P4**, and (d′) **P6** on the first cooling.

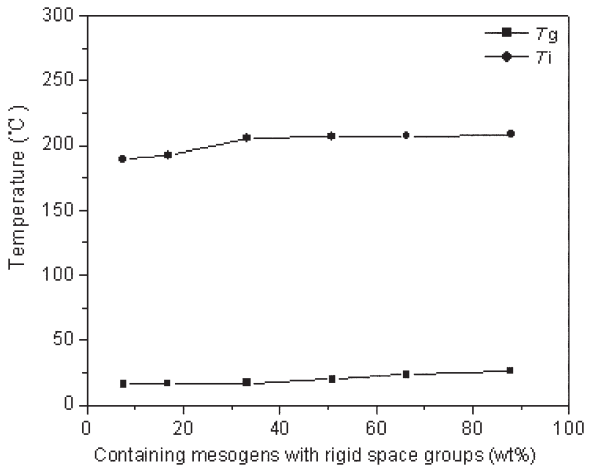

Figure 4 Effect of mesogens with rigid-space groups on the transition temperature of the LC phases in the polymer systems.

All of the polymers showed similar cholesteric phase textures in the heating and cooling cycles. The representative textures are shown in Figure 5(c,d). For polymer **P6,** when it was heated from room temperature to 30°C, the viewing field became bright. When it was heated to 187°C, the typical oily streak texture gradually appeared, and the selective reflection color changed from red to blue with increasing temperature; the texture disappeared at 208°C. When the isotropic state was cooled to 201°C, the fan-shaped focal conic texture appeared. When a mechanical force, such as slight shearing, was superimposed on the sample, the melt caused the macroscopic orientation of the cholesteric domains, and the fan-shaped focal conic texture immediately transformed into the oily streak texture, which is typical of cholesteric liquid crystals.

The cholesteric mesophase was also confirmed by X-ray diffraction. Figure 6 shows the X-ray diffraction diagrams of samples **P2** and **P4**. A broad diffraction peak around $2\theta \approx 17°$ was observed for all of the polymers, which suggested an average distance of 5 Å between two neighboring LC molecules within the layers of the mesophase. The intensity of the diffraction peak around $2\theta \approx 17°$ increased with increasing components of mesogens with rigid-space groups in polymer systems **P1–P6**, which suggested that the order between two neighboring LC molecules was disturbed by different spacers.

Reflection spectra

Cholesteric mesophases exhibit interesting optical properties, such as the selective reflection of circular

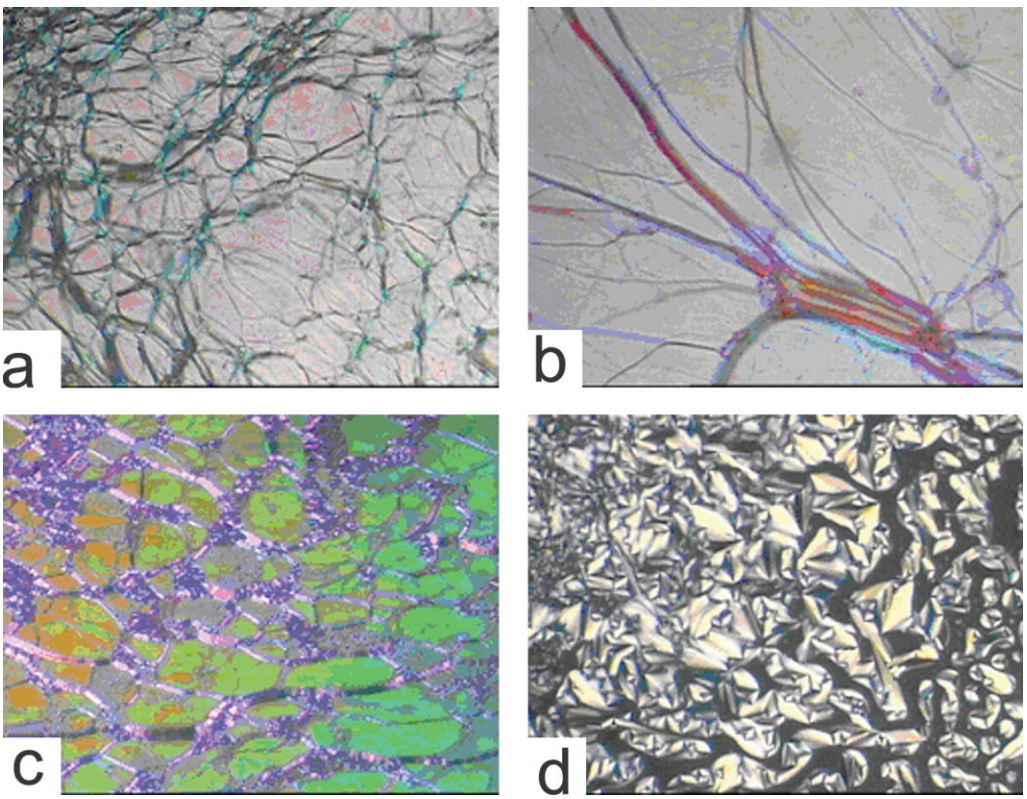

Figure 5 Optical textures of monomer **M2** and representative polymer **P6** (200×): (a) oily-streak texture of **M2** on cooling to 132°C, (b) oily-streak texture of **M2** on heating to 160°C, (c) oily-streak texture of **P6** on heating to 187°C, and (d) fan-shaped focal conic texture of **P6** on heating to 201°C. [Color figure can be viewed in the online issue, which is available at www.interscience.wiley.com.]

polarized light and an angular dependence of the reflected wavelength. If the reflected wavelength is in the visible range of the spectrum, the cholesteric phase appears colored. The wavelength of reflected light from a cholesteric sample (λ) is calculated as follows:

$$\lambda = nP \sin \varphi \quad (1)$$

where n is the average refractive index of the LC phase, P is the pitch height of the helicoidal arrangement, and φ is the incident angle of beam. P depends on many factors, such as the concentration of the chiral substance, the temperature, and an external field of mechanical, electrical, or magnetic origin.

The helical pitch is an important parameter in connection with optical properties of the cholesteric phase. Although the microscopic origins of the helical pitch are still a subject of study, it is known that the helical pitch and optical properties of side-chain cholesteric LCPs mainly depend on the polymer backbone, the rigidity of mesogenic units, the length of the flexible spacer, and the outer conditions (e.g., temperature, force field, electric field, magnetic field).

The reflected wavelengths of samples **P1–P6** were characterized with a PerkinElmer Lambda 900 instrument when the samples were heated at their mesophases (exactly 100.0°C) without any external field; these are listed in Table I. Figure 7 shows the maximum reflected wavelength of the series of

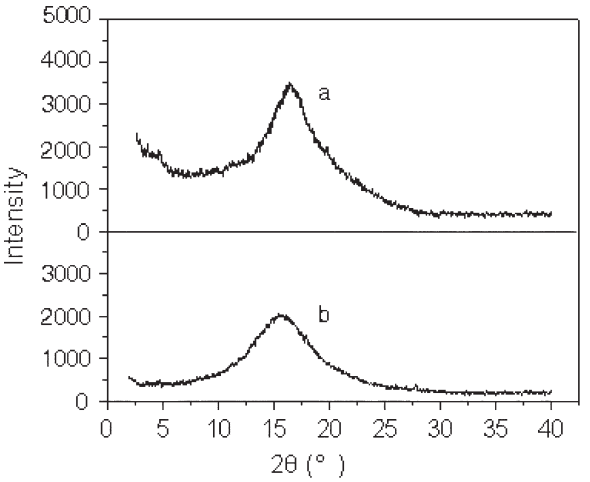

Figure 6 XRD curves of representative polymers at 125°C: (a) **P4** and (b) **P2**.

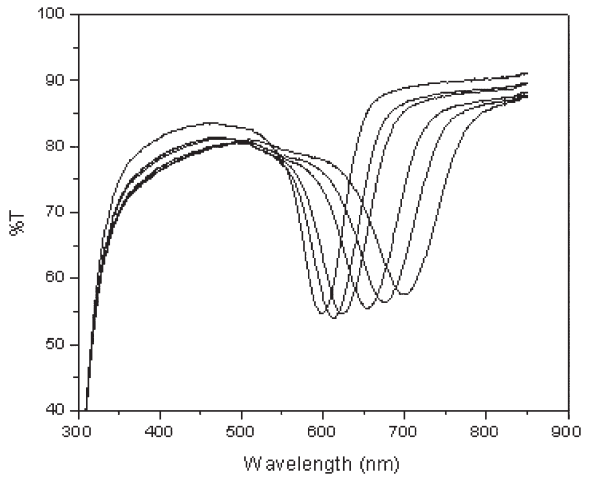

Figure 7 Selective reflection spectra of the polymer at 100°C.

polymers. The maximum reflection bands shifted to short wavelengths from **P1** to **P6** with decreasing soft-spacer components in the polymer systems, which suggested that *P* became shorter according to eq. (1).

CONCLUSIONS

A series of LC polysiloxanes were synthesized with two different cholesteric monomers. The chemical structures and LC properties of the monomers and polymers were characterized by various experimental techniques, including FTIR spectroscopy, ^{1}H-NMR, elemental analysis, DSC, and POM. The specific rotation absolute values decreased with decreasing soft spacers between the main-chain and the mesogens. All of the polymers exhibited thermotropic LC properties and revealed cholesteric phases with very wide mesophase temperature ranges. With decreasing rigid-space groups in polymers **P1–P6,** T_g and T_i increased slightly on heating cycles. Reflection spectra of the cholesteric mesophase of the series of polymers showed that the reflected wavelength shifted to short wavelength with decreasing soft-space groups in the polymers in the polymer systems, which suggested that *P* became short.

References

1. Pfeuffer, T.; Kurschner, K.; Strohriegl, P. Macromol Chem Phys 1999, 200, 2480.
2. Walba, D. M.; Yang, H.; Shoemaker, R. K.; Keller, P.; Shao, R.; Coleman, D. A.; Jones, C. D.; Nakata, M.; Clark, N. A. Chem Mater 2006, 18, 4576.
3. Yamane, H.; Kikuchi, H.; Kajiyama, T. Polymer 1999, 40, 4777.
4. Meng, F. B.; Zhang, B. Y.; Liu, L. M.; Zang, B. L. Polymer 2003, 44, 3935.
5. Sikorski, P.; Cooper, S. J.; Atkins, E. D. T.; Jaycox, G. D.; Vogl, O. J. Polym Sci Part A: Polym Chem 1998, 36, 1855.
6. Hwang, J. C.; Shu, M. C.; Lin, C. P. Macromol Chem Phys 1999, 200, 2250.
7. Lia, C. Y.; Gea, J. J.; Baia, F.; Zhanga, J. Z.; Calhouna, B. H.; Chienb, L. C.; Harrisa, F. W.; Lotzc, B.; Chenga, S. Z. D. Polymer 2000, 41, 8953.
8. Shibaev, V.; Bobrovsky, A.; Boiko, N. Prog Polym Sci 2003, 28, 729.
9. Meng, F.; Lian, J.; Zhang, B.; Sun, Y. Eur Polym J 2008, 44, 504.
10. Barmatov, E. B.; Barmatova, M. V.; Moon, B. S.; Park, J. G. Macromolecules 2004, 37, 5490.
11. Kihara, H.; Miura, T.; Kishi, R. Macromol Rapid Commun 2004, 25, 445.
12. Amabilino, D. B.; Ramos, E.; Serrano, J.; Sierra, T.; Veciana, J. J Am Chem Soc 1998, 120, 9126.
13. Ogawa, H.; Fischer, E. S.; Finkelmann, H. Macromol Chem Phys 2004, 205, 593.
14. Zhang, B. Y.; Meng, F. B.; Cong, Y. H. Opt Express 2007, 15, 10175.
15. Li, C. Y.; Cheng, S. Z. D.; Ge, J. J.; Bai, F.; Zhang, J. Z.; Mann, I. K.; Chien, L.; Harris, F. W.; Lotz, B. J Am Chem Soc 2000, 122, 72.
16. Hsu, L. L.; Chang, T. C.; Tsai, W. L.; Lee, C. D. J Polym Sci Part A: Polym Chem 1997, 35, 2843.
17. Hattori, H.; Uryu, T. J Polym Sci Part A: Polym Chem 2000, 38, 887.
18. Espinosa, M. A.; Cadiz, V.; Galia, M. J Polym Sci Part A: Polym Chem 2001, 39, 2847.
19. Carriedo, G. A.; Alonso, F. J. G.; Soto, A. P. Macromolecules 2006, 39, 4704.
20. Oda, M.; Nothofer, H. G.; Scherf, U.; Sunjic, V.; Richter, D.; Regenstein, W.; Neher, D. Macromolecules 2002, 35, 6792.
21. Zhang, B. Y.; Meng, F. B.; Zang, B. L.; Hu, J. S. Macromolecules 2003, 36, 3320.